

5. V. S. Namestnikov, "Creep beyond the elastic limit," *Izv. Akad. Nauk SSSR, Mekh. Tverd. Tela*, No. 3 (1968).
6. V. S. Namestnikov, "Creep of an aluminum alloy under variable loads," *Prikl. Mekh. Tekh. Fiz.*, No. 2 (1964).
7. V. S. Namestnikov and A. A. Khvostunkov, "Creep of duralumin under constant and variable loads," *ibid.*, No. 4 (1960).
8. V. S. Namestnikov, "Periodic creep," in: *Static and Dynamic Strength of Engineering Structures [in Russian]*, Mosk. Inst. Priborostroeniya, Moscow (1989).

DISSIPATIVE MESOSCOPIC STRUCTURES IN
PLASTIC DEFORMATION

V. V. Neverov

UDC 539.3

The studies [1-5] presented empirical proof of the existence of a new dissipative structure in thin specimens plastically deformed by shear under pressure. This so-called non-uniform-pressure structure (NPS) governs plastic motions at levels between the microscopic and macroscopic scales. Although there has been relatively little study of the processes which take place at these levels, information on them is needed to unify dislocation theory with the theory of plasticity of continua [6]. Also, events occurring at the mesoscopic level to a significant extent determine the course of friction and wear [3] and industrial processes such as mechanical fusion [4, 5].

In the present study, we examine processes involved in the creation, growth, relaxation, and plastic motion of high-pressure regions (HPR) in materials. Such regions are elements of the nonuniform-pressure structures mentioned above. We will also examine the conditions under which the latter structures are formed.

Experimental Data. Specimens 0.15-0.5 mm thick and 8-12 mm in diameter were compressed between flat parallel dies to pressures of 0.2-1.4 GPa and deformed plastically by rotation of one of the dies. Each specimen consisted either of a single metal or of three layers of two alternate metals (a sandwich). We used light microscopes and scanning and transmission (replica method) electron microscopes to study the surface of the specimens and the middle layers of the sandwiches (exposed by chemical dissolution of the outermost layers), as well as cross sections. The main findings are discussed below.

On the pre-oxidized zinc surfaces adjacent to the dies, the oxide films were displaced from some sections and concentrated in other sections (Fig. 1a, $\times 60$). The nonuniformity of the distribution of these displacements over the contact surfaces increased with an increase in shear. The material of some sections was entrained by the dies and pulled onto adjacent sections in the form of thin wedges. The wedges were lifted above the surface after the load was removed (Fig. 1b, $\times 400$).

In the specimens of ultrapure aluminum, after deformation fragments of the oxide films ended up embedded in the specimen. Thus, fragments of aluminum oxide in the form of groups of long narrow streaks (Fig. 2a, $\times 5000$) were observed on a replica from a surface exposed by layer-by-layer chemical dissolution of the specimen. When we etched the specimen in a preparation that acted selectively on the material containing oxides, deep pits that sometimes extended completely through the specimen were formed (Fig. 2, where b shows the surface of a cross section magnified 100 times and c shows the surface of the specimen magnified 170 times).

Plastic motions of the material were established from changes in the location of the oxide-film fragments (which served as reference points) and the formation of the above-

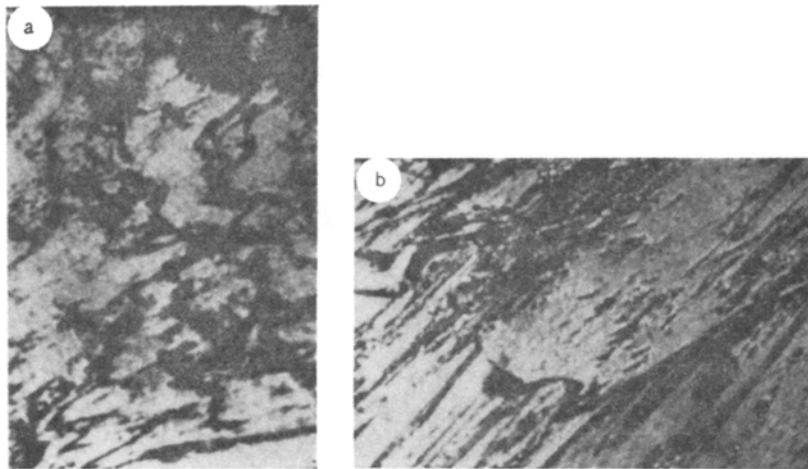


Fig. 1

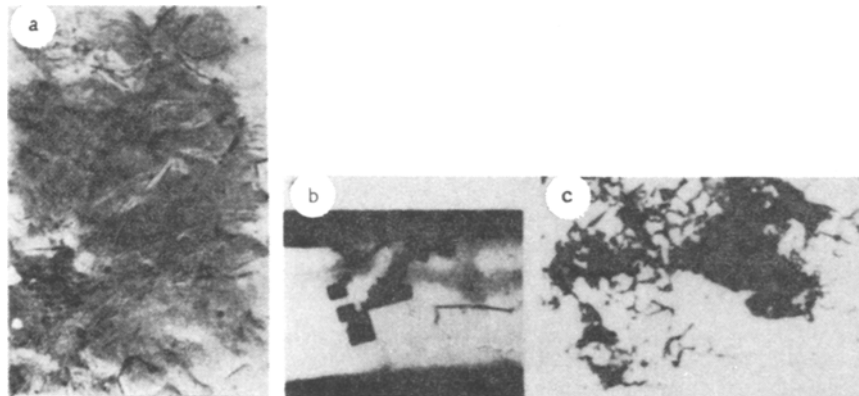


Fig. 2

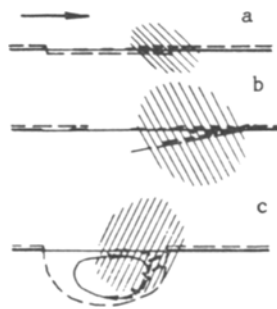


Fig. 3

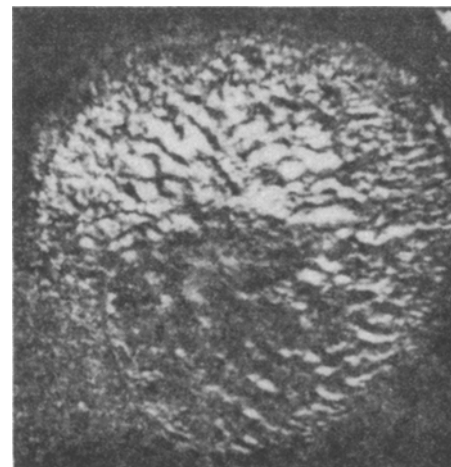


Fig. 4

mentioned wedges. The observations illustrated by Fig. 1 are schematized in Fig. 3 (a and b), while the illustrations in Fig. 2 are schematized in Fig. 3c (the arrows in Fig. 3 indicate the direction of motion of the material, the thick lines represent the oxide films, and the dashed lines show the shear localization surface). The nonuniform displacement of the material suggests that pressure was higher in those regions where the material was moved (these regions contain the above-described wedges and accumulations of oxide films, with material from the surface penetrating the bulk of the specimen). For a moderate

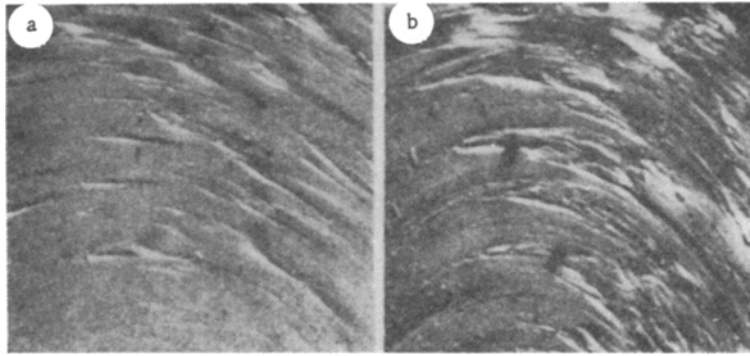


Fig. 5

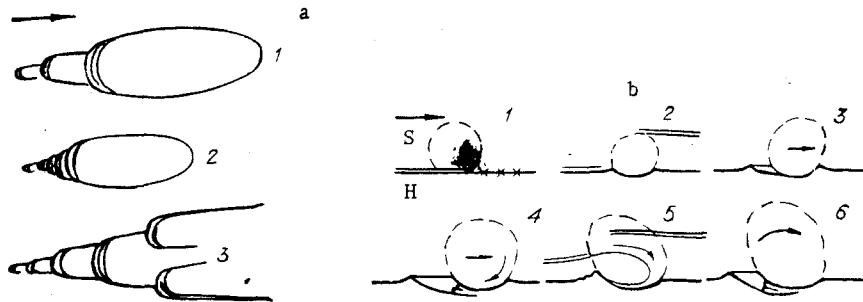


Fig. 6

wedge thickness of $2 \cdot 10^{-3}$ mm and a specimen thickness of 0.2 mm, the local increase in pressure is 1 GPa. The central parts of the HPR (the core) are hatched in Fig. 3.

A relief is formed on the surfaces of the silver middle layer in zinc-silver-zinc sandwiches during deformation (Fig. 4, overall appearance of the silver layer, $\times 14$). Scratches appear on the surface first [Fig. 5a - shear rate $\dot{\gamma} = 10^{-2} \text{ sec}^{-1}$, $\times 35$, b) $\dot{\gamma} = 1 \text{ sec}^{-2}$, $\times 35$, Fig. 6a (drawing of scratches) where 1 and 2 are for $\dot{\gamma} = 10^{-2} \text{ sec}^{-1}$ and 3 is for $\dot{\gamma} = 1 \text{ sec}^{-1}$]. The appearance of the scratches is followed by the formation of S-shaped folds (Fig. 7, where a is for $\dot{\gamma} = 10^{-2} \text{ sec}^{-1}$, $\times 35$, b is for $\dot{\gamma} = 1 \text{ sec}^{-1}$, $\times 35$, and c shows the cross section, $\times 70$). Thin bands - "tongues" - in some cases extend from the highest parts of these folds in the shear direction. The scratches are small chains of elevations connected by channels, the elevations being located at the rear end of the channels. When $\dot{\gamma} = 1 \text{ sec}^{-1}$, the channels in a given chain become broader and deeper and join with one another to cause curvature of the entire silver layer and formation of the above-mentioned folds. The folds themselves are relatively small and may intersect. When $\dot{\gamma} = 10^{-2} \text{ sec}^{-1}$, first the elevations and channels increase in size. The channels subsequently fill up with material and merge with the elevations. Despite this, some folds are formed and grow to large dimensions. These folds have smoother contours than the folds formed at higher shear rates.

The sandwiches consisted of layers of metals strain-hardened to the maximum extent possible. The microhardnesses of the zinc and silver were 0.5 GPa and 1.0 GPa, respectively. These figures correspond to $\tau_{\text{Szn}} = 0.09 \text{ GPa}$ and $\tau_{\text{SAg}} = 0.17 \text{ GPa}$. The plastic strain was initially concentrated in the metal with a smaller value of τ_{S} , i.e., in the zinc. The scratches on the silver showed that shear strains also took place along the contacts between the layers of the sandwich. The zinc had regions in which τ_{S} was higher than in the corresponding silver and increased by a factor of at least two. These strain-hardened regions were acted upon by a force normal to the contact surface. This force created a higher-than-average local pressure equal to at least the microhardness of silver, i.e., no lower than 1 GPa. It is natural to assume that this pressure also increased the value of τ_{S} in the region.

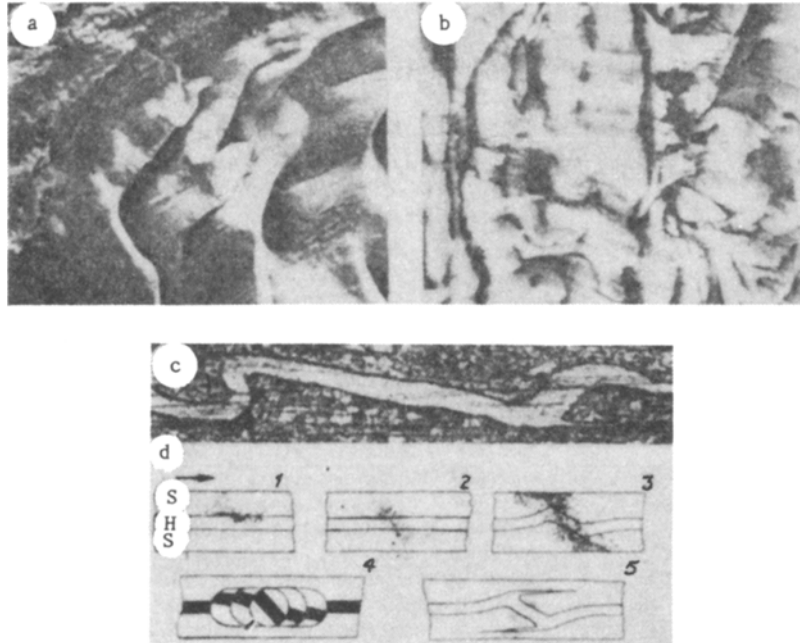


Fig. 7

It follows from the formation of the folds (Fig. 7) that regions of the sandwich spanning the entire height of the specimen underwent rotation. Moreover, since elements of the silver layer were sometimes rotated relative to their initial position without a change in layer thickness, the regions (or their central parts, at least) underwent these rotations as a single entity. The axes of rotation were close to the radial direction, while the motions were similar to the rolling that would have been imparted to a roller placed between the surfaces of the dies. Since the area of the surfaces accompanying the shear rotations was greater than in the case of the alternative "quasi-laminar" shear and since the rotation induced plastic motion of a metal (silver) that was stronger than a metal in which the alternative shear could have taken place, we can assume that the given region was acted upon by locally increased forces and that the zinc was strain-hardened in the rotation region by the compressional stress.

Allowing for the above, in Fig. 6b we have schematized variants of plastic motion leading to the formation of scratches. The letters S and H denote soft and hard layers. The HPR is either hatched or surrounded by dashed lines. The double lines represent shear-localization surfaces, while the x's represent locks, i.e., sections in which shear over the contact surfaces of the layers is moderated. Scratches are formed as a result of the alternation of shears and rotations of the cores of the HPRs as a whole in the zinc (Fig. 6b, where 1 and 2 denote the formation of the cores, 3 denotes shearing, 4 and 5 denote rotation, and 6 denotes core growth). The silver is drawn under the core in a rotating motion, with the consequent formation of elevations at the rear ends of the channels.

The sketches in Fig. 7d illustrate stages in the formation of a fold (1 and 2 denote the formation of an HPR, 3 and 4 denote rotations, and 5 denotes the final configuration).

The fact that the elevated regions comprising the scratches (and resulting from crushing of the material) remain intact after being passed over by the material behind the core suggests that the core takes up the compressive force from the dies. Thus, pressure is reduced in the material surrounding the core, and the zinc behind the core may lose contact with the silver. This in turn reduces the mechanical load on the elevations, leaving them intact. A similar phenomenon - the separation of compressed friction surfaces as a result of their splitting by material accumulated at different sites - was seen in [7]. Since the length of a chain of elevations is 2-3 times greater than the width of the corresponding channel, if we assume that the linear dimensions of the core are equal to the width of the channel we find that local pressure in the core is 3-4 GPa for a mean pressure of 1 GPa on the die.

The flattening of the channels in the case of low-rate deformation shows that the rates of the processes that lead to strengthening and enlargement of the HPR decrease with

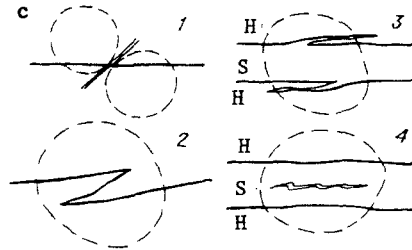
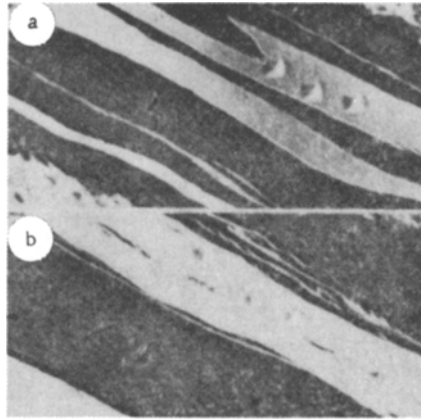


Fig. 8

a decrease in γ . Thus, the pressure gradients are made smaller by relaxation. Judged from the time over which the channels of the scratch are staved in, relaxation time is several seconds. Since folds are still formed, however, it follows that their precursors are longer regions with a lower excess pressure. These regions disappear in the course of evolution of the marks on the silver. The interpretation of events just given is consistent with the large dimensions and smooth contours of the folds (Fig. 7a and b). It should also be noted that convergence of the channels is precluded as a reason for the formation of scratches from dust particles or other extraneous inclusions.

The evolution of the shape of the layers of the sandwich and the associated plastic motions depend on the ratio of the shear strengths of the outermost and middle layers f . This is true for $f = 0.5$. If $f = 1$, the amplitude of the folds decreases and interference regions with long bands become predominant (Fig. 8a, $\times 14$). If $f > 1$, periodic thickenings are formed on the soft middle layer. Very thin bands may extend into the solid layer from these thickened zones, with several bands emanating from one site. Thin discontinuities may be formed along the middle part of the soft layer. Small folds can form on these discontinuities (Fig. 8b, $\times 14$). The corresponding plastic motions are schematized in Fig. 8c, where 1 and 2 represent the formation of an interference region, 3 shows the formation of bands, and 4 denotes cutting of the HPR in the diameter direction. The core of the HPR is bounded by dashed lines.

The above observations and analysis lead to the following conclusions. The shear strains are distributed unevenly over the contact surfaces, causing a redistribution of the material and, thus, redistributions of density and pressure. The pressure in an HPR may reach several gigapascals, which significantly increases the value of τ_s for the material of the region. Since the HPR has been strengthened, it undergoes plastic shears and rotations primarily as a unit hole. Taking place simultaneously with the pumping processes are relaxation processes. The HPRs grow if the former predominate (high $\dot{\gamma}$, low temperatures). Competition between these processes results in ordering of the HPRs and the formation of a dynamic dissipative nonuniform-pressure mesostructure.

Since it is almost impossible to eliminate local discontinuities of the acting stresses and τ_s , plastic strains will always be nonuniform in character. Thus, in principle, NPSs always develop in a material, and the only question is the extent of their development and their effect on deformation compared to the effects of the factors normally considered.

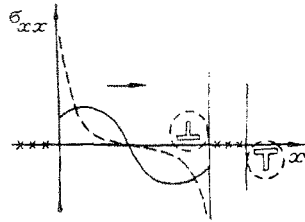


Fig. 9

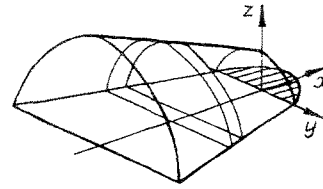


Fig. 10

TABLE 1

x/l	β, deg					
	20			5		
	σ_{xx}/σ_s	F/F _s	M/M _s	σ_{xx}/σ_s	F/F _s	M/M _s
1	1,11	3,3	5,7	1,14	1,66	1,8
2	1,23	12	39	1,39	3,2	4,9
5	1,31	28	126	1,61	5,6	11
10	1,46	98	810	2,15	16	45
15	1,55	217	2560	2,55	34	124

Initiation of a HPR. The stresses acting on the contacts between the layers form a mosaic. For example, loading of the material in elastic shear is retarded ahead of local contact sections with a high friction coefficient, i.e., sections with a lock (represented by the x's in Fig. 9). The value of σ_{xx} ahead of the lock increases in this case (the solid curve in Fig. 9). There is also an increase in $\sigma_{yy} = \nu\sigma_{xx}$ (where ν is the Poisson's coefficient). Thus, the shear stresses $\tau_f = \mu\nu\sigma_{xx}$ also increase (where μ is the friction coefficient). At this stage, the process is similar to the formation of jams in steam driving, when a layer of logs lies flat on the bottom of the pile in front of a relatively weak obstacle and increases the restraining force. Thus, σ_{xx} increases with increasing distance from the lock. Assuming that the HPR has the form of a truncated half-cone in front of the lock and that part of the apex of the cone rests on the lock (Fig. 10, where the lock is darkened), we obtain the following from the condition of equilibrium of the layer dx if we assume that $\sigma_{xx} = \text{const}$ in the sections $x = \text{const}$

$$\frac{\sigma_{xx}}{\sigma_s} = \left(1 - \frac{2 \operatorname{tg} \beta x}{l}\right)^{4\mu\nu/(\pi \operatorname{tg} \beta)}, \quad (1)$$

where σ_s represents the stresses in front of the lock; β is the cone angle; l is the size of the lock. Table 1 shows results of the use of (1) to calculate the relative quantities σ_{xx}/σ_s , F/F_s, and M/M_s (where F is the force acting in the section $x = \text{const}$ and M is the resulting moment). If we assume that the areas of the lock and the cross section of the HPR at the lock are the same and that the force resisting shear of the lock alone is equal to the amount by which the shearing force on the lock exceeds the mean value, we obtain $\sigma_s = \Delta\mu p$ (where $\Delta\mu$ is the increase in the friction coefficient on the lock and p is the mean pressure). We find that $\sigma_s = 0.1$ GPa for $\Delta\mu = 0.1$ and $p = 1$ GPa and that, in accordance with the data in Table 1, σ_{xx} increases only slightly.

With the development of plastic shear strain over the contact between the layers, the distribution of σ_{xx} is gradually transformed from elastic to plastic (the dashed curve in Fig. 8). This development is similar to that which takes place in the case of a two-sided pile-up of edge dislocations [8]. Thus, stress concentration increases ahead of the lock. If we assume that the force acting in the elastic state in the section $x = -5l$ is now taken up by the section $x = -l$, then on the basis of the data in Table 1 we find $\sigma_{xx} = 0.8-3.3$ GPa. This result is close to the experimental data.

Thus, nonuniformity of the plastic motions occurring near the lock results in the creation of a core of highly compressed material which serves as the foundation of the HPR. This core may undergo shears and rotations as a single entity under the influence of F and M.

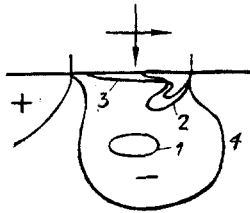


Fig. 11

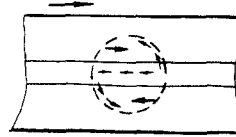


Fig. 12

Strain-hardening of the Material of the HPR. We know of two groups of experiments that have been performed to examine the effect of pressure on τ_s . In the first group, plastic deformation was realized by tension in a pressure-transmitting fluid with relatively low strain rates $\dot{\epsilon} \sim 10^{-4}$. The effect of pressure was explained in terms of an increase in the elastic moduli and was described by the formula [9]

$$\tau_s = \tau_{s0} [1 + (6-11)p/K], \quad (2)$$

where τ_{s0} is the maximum shear strength without pressure; K is the bulk modulus.

In the second group of experiments, deformation took place by shear under pressure with a shear rate of about 1 sec^{-1} . The most accurate results were obtained in tests conducted with annular dies [10, 11]. The increment of τ_s was several times greater in this case and was described by the formula

$$\tau_s = \tau_{s0} + kp \quad (3)$$

(where k is a coefficient equal to 0.05-0.10 for different metals). Shear strain intensity and shear strain rate were much greater for the second group than for the first. This means that (3) accounts for both the increase in the moduli and the additional strain-hardening which takes place. The latter [12] is related to refinement of the grains and fragments of the material. Since the HPR develops in soft metal - where the plastic strain is initially concentrated - Eq. (3) is used for this metal and Eq. (2) is used for the hard metal. Thus, for example, the condition $\tau_{sZn} = \tau_{sAg}$ is satisfied at $p = 2.3 \text{ GPa}$. The force which forms the core creates high stresses that act on the hard metal from the soft metal on the side of the core. The core is pressed into the hard layer and involved in plastic motions.

Configuration of the Stress Field of the Core. After cores are formed, the stress field in the specimen can be conveniently divided into two parts: the mean compressional stress and the local fields due to forces concentrated on the areas of contact between the cores and the hard layer. The local fields can be represented on the basis of the solution of the problem of the stresses in an elastic half-space from normal and tangential loads distributed along a rectangular region [13]. The position of the region in which the intensity of the shear stresses is maximal changes with an increase in the ratio of the tangential force to the normal force. This ratio alternately equals 0, 0.2, and 0.4 along lines 1-3 in Fig. 11. There is a corresponding change in the position of the surface over which plastic shear develops in the core. Since the solution in [13] obtained on the basis of the elastic characteristics of the material contains Poisson's ratios that change only slightly for different metals, similar fields exist within each layer and shear can take place in any layer in relation to the τ_s calculated with allowance for the effect of pressure (Fig. 11, where the number 4 represents the line of equal principal normal stresses).

Pumping and Relaxation Processes. Table 2 shows estimates of the rate of increase in pressure (dp/dt) in the HPR for several mechanisms of redistribution of the material. In each case, dp/dt is inversely proportional to the size of the core L . Thus, if no allowance is made for other circumstances, p is larger, the smaller L .

Table 3 presents motion diagrams along with equations and characteristics of processes involved in the plastic relaxation of cores. In the first process, material is removed from the core by the diffusion of vacancies into the core. Since relaxation time t_e is much longer than the test time in this case, the mechanism responsible for relaxation cannot be purely diffusional. Here, relaxation is controlled by diffusional-dislocational and (or) dislocational mechanisms. The second process involves axial displacement of material from the core (which is assumed to be cylindrical in this case) under the influence of uniform

TABLE 2

Process	Figure	Formulas to estimate the rate of change in pressure with $\dot{\gamma} = 1 \text{ sec}^{-1}$ and the chosen variables	$\frac{dp}{dt}$, GPa/sec
Retardation of shear at a lock	6, a, b, 1	$\frac{dp}{dt} = K \frac{\Delta V}{V} \frac{v}{\Delta b} \approx K \frac{v}{L}$, $K_{Zn} = 60 \text{ GPa}$, $v = 4 \cdot 10^{-4} \text{ m/sec}$ $\Delta V = \Delta b L$, $V = L^2$, $L = 10^{-4} - 10^{-6} \text{ m}$	240—2400
Misalignment of slip planes	6, b, 2, 5	$\frac{dp}{dt} = K \frac{s}{L} \frac{v}{L}$, $s/L = 0.2$, $v/L = 0.4 - 4 \text{ sec}^{-1}$	48—480
Rotation of a non-equiaxed core	6, b, 5, 6 7, d, 2—4	$\frac{dp}{dt} \approx K \frac{L_1 - L_2}{L_1 \sqrt{2}} \frac{v}{L_1}$, $L_1 - L_2 = 0.2 L_1$	30—300
Formation of thin interlayers	8, c, 3	$\frac{dp}{dt} = K \frac{L_l}{L} \frac{v}{L}$, $L_l/L = 0.1$	24—240
Movement of cores onto one another	7, d, 2, 3 8, c, 1	$\frac{dp}{dt} = K \frac{\Delta L}{L} \frac{v}{L}$, $\Delta L/L = 0.2$	48—480
Shear in a plane not parallel to the macroscopic shear plane	8, c, 2	$\frac{dp}{dt} = K \frac{b \operatorname{tg} \alpha}{L} \frac{v}{b}$, $\alpha = 0.1$	24—240

Note. v is the shear rate; Δb is retarded shear; s is the distance between shear planes; $L_{1,2}$ are the dimensions of the core in mutually perpendicular directions (it is assumed that they are extreme); L_l is the thickness of an interlayer; ΔL is the overlap of the cores; b is the shear strain; α is the angle between the microscopic and macroscopic shear planes.

lateral pressure. It is assumed that the process is similar to the tension of a cylinder. Proceeding on this basis, we further assume that the amounts of work done in tension and compression are equal. Since the displacement occurs into the surrounding material, the flow stress is doubled. This condition was also adopted in subsequent models. In the third case, the pressure corresponding to the beginning of plastic deformation was found for a scheme of motion involving flattening of the core under the influence of σ_{zz} , while t_e was found for the displacement of layers parallel to the xOy plane in the direction of the macroscopic shear vector. The fourth process involves telescopic flow caused by a drop in lateral pressure from the middle part of the core — from the cylinder toward to end. In this case, the central part of the core remains in the elastic state. This is reflected by the graph.

It follows from these results that the largest static local pressure gradients for roughly equiaxed cores is about $0.8H$, where H is the microhardness of the metal ($H_{Zn} = 0.5 \text{ GPa}$, $H_{Ag} = 1 \text{ GPa}$). Since the pressure in the cores is greater than these values, the NPS is dynamic and requires continuous pumping to be sustained.

For low rates of deformation along the lines (Fig. 5a), the lifetime of the cores $t_1 = 10-100 \text{ sec}$. The time of growth of the cores until they begin to compete with one another at high shear rates, determined along the lines until their intersection (Fig. 5b), is $t_2 = 1-5 \text{ sec}$. Estimates made of t_e for processes 2 and 4 are consistent with these values: $t_1 > t_e > t_2$. The value of the viscosity coefficient η for zinc used to obtain the estimates in Table 3 agrees with the data in [9].

TABLE 3

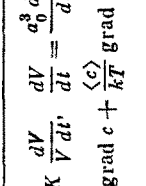
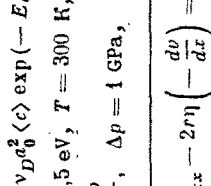
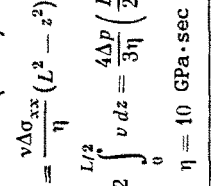
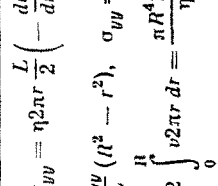
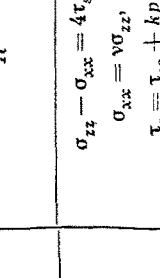
Motion diagram	Yield-point condition equilibrium condition	characteristics of the plastic transition	Viscous flow kinetic equation	relaxation time, sec
			$\frac{dP}{dt} = K \frac{dV}{V} \frac{dN}{dt} = \frac{\sigma_0^3 dN}{dt}$ $\frac{dN}{dt} = D \left(\text{grad } c + \frac{\langle c \rangle}{kT} \text{ grad } U \right) S n_0$ $D = \frac{1}{6} v D_0^2 \langle c \rangle \exp(-E/kT)$ <p>$\langle c \rangle = 10^{-5}$, $E = 0.5$ eV, $T = 300$ K, $D = 10^{-13}$ cm, grad $U \approx \frac{\sigma_0^3 \Delta p}{R}$, $\Delta p = 1$ GPa, $R = 10^{-6}$ m</p>	<p>10⁵</p>
	<p>$dA_{\text{compr}} = dA_{\text{tension}}$ $2\pi R L p dR = 2\pi R^2 \sigma_s dL$ $dV = 0, 2 \frac{dR}{R} = -\frac{dL}{L}$</p>	<p>$P_{Zn} = 0.4$ GPa $P_{Ag} = 0.8$ GPa</p>	$2z \Delta \sigma_{xx} - 2r \eta \left(-\frac{dv}{dx} \right) = 0$ $v_x = \frac{v \Delta \sigma_{xx}}{\eta} (L^2 - z^2)$ $\frac{dV}{dt} = 2 \int_0^{L/2} v dz = \frac{4 \Delta p}{3 \eta} \left(\frac{L}{2} \right)^2$ <p>$\eta = 10$ GPa·sec</p>	<p>1</p>
	<p>$\sigma_{zz} - \sigma_{xx} = 4\tau_s$ $\sigma_{xx} = v \sigma_{zz}$ $\tau_s = \tau_{s0} + k p$ $p = \frac{1+v}{2} \sigma_{zz}$</p>	<p>$\sigma_{zz Zn} = 0.4$ GPa, $\sigma_{zz Ag} = 0.9$ GPa</p>	$\pi R^2 2v \Delta p = 2\pi R \frac{L}{2} \tau_s$ <p>$p = 0.5 p_{\text{max}}$ $\frac{R}{L} = \frac{1}{\Delta p} \left[\tau_{s0} + k \frac{2(1+v)}{3} p \right]$</p>	<p>5</p>
			$\pi r^2 \sigma_{yy} = \eta 2\pi r \frac{L}{2} \left(-\frac{dv}{dr} \right)$ $v = \frac{\Delta \sigma_{yy}}{\eta L} (l^2 - r^2), \quad \sigma_{yy} = 2v p,$ $\frac{dV}{dt} = 2 \int_0^R v 2\pi r dr = \frac{\pi R^4 2v \Delta p}{\eta L}$	

TABLE 4

Ensembles	Formulas	Pressure, GPa	
		0,5	1
Edge dislocation	$p_1 = \frac{2(1+\nu)Gb \sin \theta}{6\pi(1-\nu)r}$ $\nu = 0,3, G = 40\text{GPa}, b = 0,3 \text{ nm}$	4,6	2,3
Planar pile-up of $n = 10$ edge dislocations	$p_n \approx np_1$	46	23
Pile-up of $n = 10$ prismatic dislocations with a loop radius equal to the length of the pile-up L_p	$p \approx 2p_n + p_{\text{interact}} \approx 2np_1 +$ $+ \frac{n^2Gb^2}{L_p 2\pi(1-\nu)r}$	100	50

Plastic Motions of the Core. The schemes depicted in Figs. 6b, 7d, and 8c show that cores may be cut over a surface which intersects it near either its boundary (Fig. 6b, 5, 8c, 3) or over a diameter (Figs. 8c, 1, 2, 4). Here, the core may undergo plastic translational (Figs. 6b, 3, 4) and rotational (Figs. 6b, 4-6, 7d, 3, 4) motions as a whole. The character of plastic motion of the core is determined by the acting τ and limiting τ_s stresses; τ depends on the configuration of the stress field. If the core is smaller than the thickness of the layer, this configuration is described by the solution obtained in [13] (Fig. 11). The value of τ_s depends on the location of the hard and soft components and on p . The general rule is that motion of the core as a single entity is more likely, the greater the value of p and, thus, τ_s .

As an example, we will examine the conditions for a change in the motion of a core from rotation as a whole to shear as a whole (Fig. 6a and b), as well as from rotation as a whole to shear over a diametrical plane (Fig. 6b, 4, 8c, 4). In the first case, the depth of the channel increases as shear proceeds. Thus, there is also an increase in the forces acting parallel to the vector of macroscopic shear, the size of the core, the force arm, and the turning moment. The result is the replacement of shear by rotation. Here, the core is lifted out of the channel, the force resisting shear decreases, shearing begins anew, the core is embedded, etc.

To evaluate the conditions under which there is a change in the type of motion in the second case, we assume in the plane scheme (Fig. 12) that the core has the form of a circle acted on by a couple F with an arm equal to the radius of the circle R . We further assume that reactive stresses τ_{sp} act on the surface of the core in the first and third quadrants to prevent rotation. In the second and fourth quadrants, the material surrounding the core moves together with it (resulting in an increase in both the size of the core and the pressure in it). Here, the core may be sheared in the diameter direction, where resistance to shear is equal to τ_{sd} . Then we have the following for the turning moment M required for rotation and the force F_d required for shear

$$M = FR = \tau_{sp}\pi R^2; \quad (4)$$

$$F_d = \tau_{sd}2R. \quad (5)$$

Equating F and F_d and inserting (5) into (4), we obtain

$$\tau_{sd} \cong 1,57\tau_{sp}, \quad (6)$$

where the first sign corresponds to shear and the second corresponds to rotation. In a material with uniform properties $\tau_{sd} = \tau_{sp}$, and shear takes place in accordance with (6). An increase in rotation is facilitated by the fact that τ_{sd} increases under the influence of pressure and by the fact that a layer of material with a high value of τ_s is located in the middle part of the core. In fact, as described above, rotations predominate at $f < 1$ while shears predominate at $f \geq 1$.

Conditions of NPS Formation. Any disturbances of the laminar character of the plastic motions contribute to the formation of high-pressure regions. Examples of such disturbances include differences in the direction of normals to the slip planes and the shear vectors in adjacent volumes, nonuniformity of the stresses on the contact surface between the specimen and the tool, etc. Since it is impossible to completely eliminate nonuniformities in the acting stresses and (or) τ_s , high-pressure regions are always created in the plastic deformation of solids. Table 4 shows formulas that can be used to estimate hydrostatic pressure $p = (1/3)(\sigma_{xx} + \sigma_{yy} + \sigma_{zz})$ and the dimensions of HPRs for several dislocation configurations [8]. It should be pointed out that the nucleation of cracks - which has been studied repeatedly - and the creation of high-pressure regions are one and the same process - a redistribution of material in a body undergoing plastic deformation. New HPRs are an obstacle to subsequent shear and thus grow at an accelerated rate.

A nonuniform-pressure structure is formed if the rate of plastic deformation is greater than the critical value, so that the pumping rate exceeds the rate of relaxation. The critical rate depends on the test conditions and the properties of the material being deformed. In connection with this, let us briefly discuss one of the factors that affects the critical rate: the number of parallel (in terms of their possible contribution to large-scale deformation) channels in which small-scale plastic motions develop. We will call this parameter the number of plastic degrees of freedom and designate it as i . We conditionally assume the existence of three scales of plastic motion (macro-, meso-, and micro-levels). We further assume that pumping processes in the material are controlled by the mechanisms responsible for plastic motions at the meso-level - with i_1 - while relaxation processes are controlled by the mechanisms active at the micro-level - with i_2 . The greater i_1 , the more likely it is that a second channel will become active if a given channel is blocked by the formation of an HPR on it. In this case, pumping stops in the HPR on the first channel and the region undergoes relaxation. The higher i_2 , the greater the probability of relaxation. Thus, a decrease in both i_1 and i_2 helps reduce the critical rate. It follows from this that the formation of NPSs is facilitated by the following: a decrease in the number of easily activated slip systems; an increase in the anisotropy of τ_s ; a predisposition to shear localization in the material; plastic constraint (such as near the surface of contact of the specimen with the harder tool); a decrease in specimen thickness in the case of such contact; the presence of inclusions with a high τ_s in the specimen, etc. For thin three-layer specimens [1, 2], the critical rate $\dot{\gamma} \approx 10^{-3} \text{ sec}^{-1}$. A nonuniform-pressure structure is formed at $\dot{\gamma} \sim 1 \text{ sec}^{-1}$ in high-purity (99.9996 at. %) aluminum recrystallized at room temperature and subjected to deformation under the same conditions as described in [1, 2].

Dissipative structures formed in plastic deformation must be functionally stable, i.e., the plastic motions they induce must not (at least rapidly) disturb elements of the structure itself. The stability of the NPS is determined by the extent to which it induces motion of the HPR as a whole. Thus, the functional stability of the NPS will be greater, the more developed it is and the higher the pressure in the HPR.

Taking into account the rapid growth of the HPR and the viscoplastic character of the relaxation process, we write the unidimensional kinetic equation for the difference between the local and mean pressures Δp in the form

$$\frac{\partial(\Delta p)}{\partial t} = a\Delta p + \frac{c}{\eta} \frac{\partial^2(\Delta p)}{\partial x^2}, \quad (7)$$

where a is the acceleration factor, taken to be proportional to the shear rate; $C \approx 1$. The steady-state solution describes a periodic change in Δp with the wavelength $\lambda_s = 2\pi(a\eta)^{0.5}$. Random discontinuities with $\lambda < \lambda_s$ relax, while those with $\lambda > \lambda_s$ become more intense. Taking $\eta = 20 \text{ GPa}\cdot\text{sec}$ for zinc [9], $a = 2 \text{ sec}^{-1}$ for $\dot{\gamma} = 1 \text{ sec}^{-1}$ and $a = 2 \cdot 10^{-2}$ for $\dot{\gamma} = 10^{-2} \text{ sec}^{-1}$ we find that $\lambda_s = 0.03 \text{ mm}$ when $\dot{\gamma} = 1 \text{ sec}^{-1}$ and $\lambda_s = 0.3 \text{ mm}$ when $\dot{\gamma} = 10^{-2} \text{ sec}^{-1}$. The mean distances between S-shaped folds seen in [2] are greater than the indicated values, which is consistent with (7).

In conclusion, we note that materials with a structure and, thus, with ductility properties similar to those acquired by a homogeneous material due to the formation of nonuniform-pressure structures are common in nature and technology. Among them are composite materials, mortars with a filler, sands, etc., i.e., materials that can be regarded as consisting of two subsystems with different τ_s .

LITERATURE CITED

1. V. V. Neverov and P. P. Zhitnikov, "Rotations of a material during the shearing plastic deformations of thin layers," *Izv. Vyssh. Uchebn. Zaved., Fiz.*, No. 2 (1989).
2. V. V. Neverov, P. P. Zhitnikov, and V. V. Gorkavenko, "Formation of high-pressure regions during plastic deformation," *ibid.*, No. 6 (1990).
3. V. V. Neverov and V. G. Supess, "Mechanism of embedding of surface films during the action of large normal loads and shear strains," *Trenie Iznos*, 12, No. 3 (1991).
4. V. V. Neverov and P. P. Zhitnikov, "Processes involving the formation of compounds during the plastic deformation of binary mixtures of metals," *Fiz. Met. Metalloved.*, No. 11 (1990).
5. V. V. Neverov, "Dissipative 'sandy' structures associated with plastic deformation and kinetic features of mechanical fusion," *ibid.*, No. 1 (1992).
6. V. E. Panin, Yu. V. Grinyaev, V. M. Danilov, et al., *Structural Levels of Plastic Deformation and Fracture [in Russian]*, Nauka, Novosibirsk (1990).
7. M. Cocks, "Role of displaced metal in the sliding of flat metal surfaces," *J. Appl. Phys.*, 35, No. 6 (1964).
8. J. Hirth and I. Lote, *Theory of Dislocations [Russian translation]*, Atomizdat, Moscow (1972).
9. G. J. Frost and M. F. Eshelby, *Maps of Deformation Mechanisms [Russian translation]*, Metallurgiya, Chelyabinsk (1989).
10. P. I. Ogibalov and I. A. Kiiko, *Essays in High-Parameter Mechanics [in Russian]*, Izd. MGU, Moscow (1966).
11. S. Erbel, "Metoda wyznaczania krzywej umocnienia dla bardzo dużych odkształceń," *Mechanik*, 39, No. 10 (1966).
12. V. A. Zhorin, V. V. Fedorov, D. K. Khalimova, et al., "Formation of an ultrathin structure in titanium nickelide during plastic deformation at high pressure," *Dokl. Akad. Nauk SSSR*, 275, No. 6 (1984).
13. M. M. Saverin, *Contact Strength of a Material Loaded Simultaneously by Normal and Shear Loads [in Russian]*, Mashgiz, Moscow (1946).